Supporting Information

Preparation and application of in situ polymerization self-assembly conductive ceramic membranes via graphene/carbon nanotube/polypyrrole

Xinling Wang [a], Chunhui Zhang [a*], Zong Liu [a b], Bingxu Quan [a], Wenjing Lu [a], Xuezhi Li [a], Peidong Su [a*], Yuanhui Tang [a], Yuanqing Bu [c], Rong Zhou [c]

[a] College of Chemistry and Environmental Engineering, China University of Mining and Technology, Beijing 100083, China;

[b] Beijing Tianma Intelligent Control Technology Co., Ltd. Beijing 101399, China;

[c] Key Laboratory of Pesticide Environmental Assessment and Pollution Control, Nanjing Institute of Environmental Science, Ministry of Ecology and Environment, Nanjing, China;

* Correspondence: Room 607, Yifu Science & Research Building, Ding 11 Xueyuan Road, 100083, Beijing, China. Tel/fax: +86 10 6233 9331; Chunhui Zhang.

2 Tables

5 Figure

23 **Table 1** Analysis of Variance for Quadratic model of square resistance

Source	Sum of Squares	df	Mean Square	F-value	Prob>F
Model	1.088E+006	9	1.209E+005	14.25	0.0010
A-GO-CNTs doping amount	37531.15	1	37531.15	4.30	0.0735
B- oxidation polymerization time	1.413E+005	1	1.413E+005	16.66	0.0047
C-Py concentration	5.496E+005	1	5.496E+005	64.80	< 0.0001
AB	3918.76	1	3918.76	0.46	0.5185
AC	5704.03	1	5704.03	0.67	0.4392
BC	1.241E+005	1	1.241E+005	14.63	0.0065
A^2	27.40	1	27.40	3.231E-005	0.9563
B^2	36323.71	1	36323.71	4.28	0.0773
C^2	1.786E+005	1	1.786E+005	21.05	0.0025

24

Table S2 Analysis of Variance for Quadratic model of membrane pure water flux

Source	Sum of Squares	df	Mean Square	F-value	Prob>F
Model	57869.61	9	642.96	157.99	< 0.0001
A-GO-CNTs doping amount	1262.53	1	1262.53	31.02	0.0008
B- oxidation polymerization time	23620.51	1	23620.51	580.37	< 0.0001
C-Py concentration	25969.20	1	25969.20	638.07	< 0.0001
AB	71.40	1	71.40	1.75	0.2269
AC	0.25	1	0.25	6.143E-003	0.9397
BC	0.090	1	0.090	2.211E-003	0.9638
A^2	4258.52	1	4258.52	104.63	< 0.0001
B^2	120.63	1	120.63	2.96	0.1288
C^2	2061.58	1	2061.58	50.65	0.0002

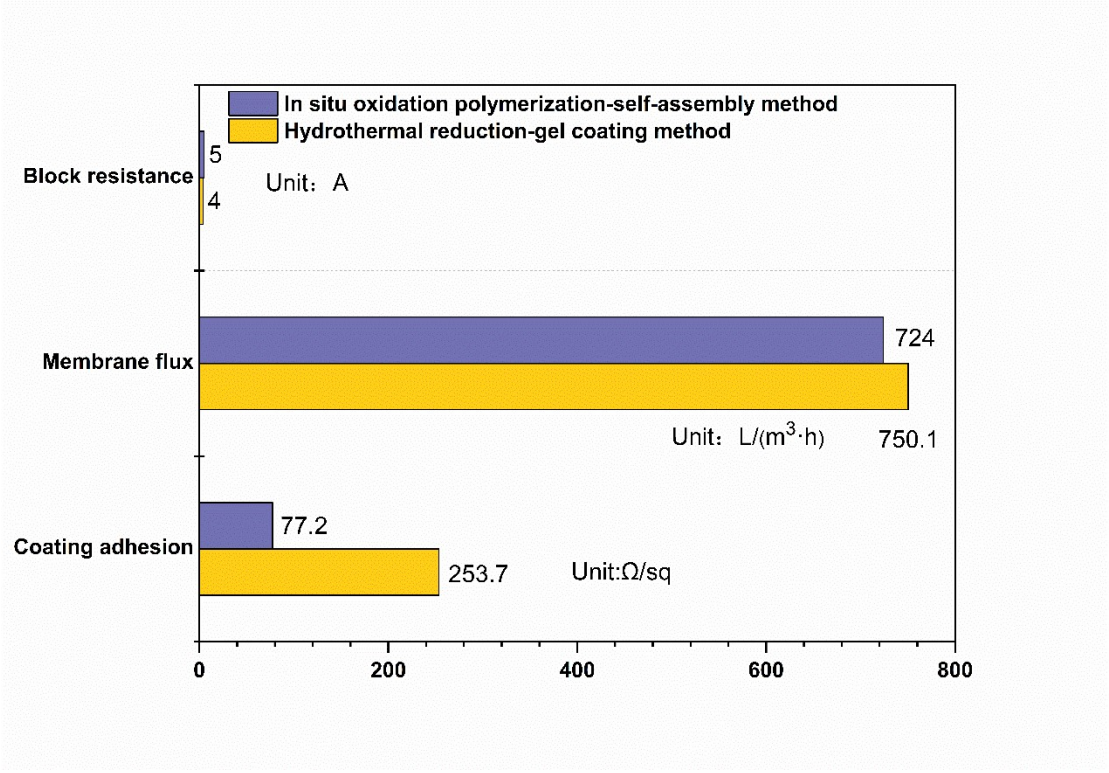

27

28 **Fig. S1.** The properties of membrane materials under different preparation methods

29

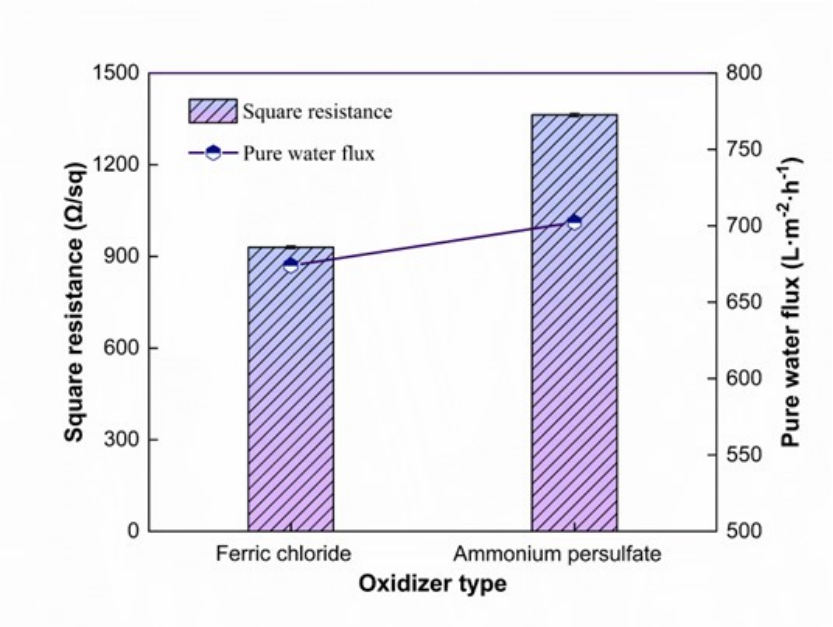

Fig. S2 Effect of oxidant types on the properties of membrane materials.

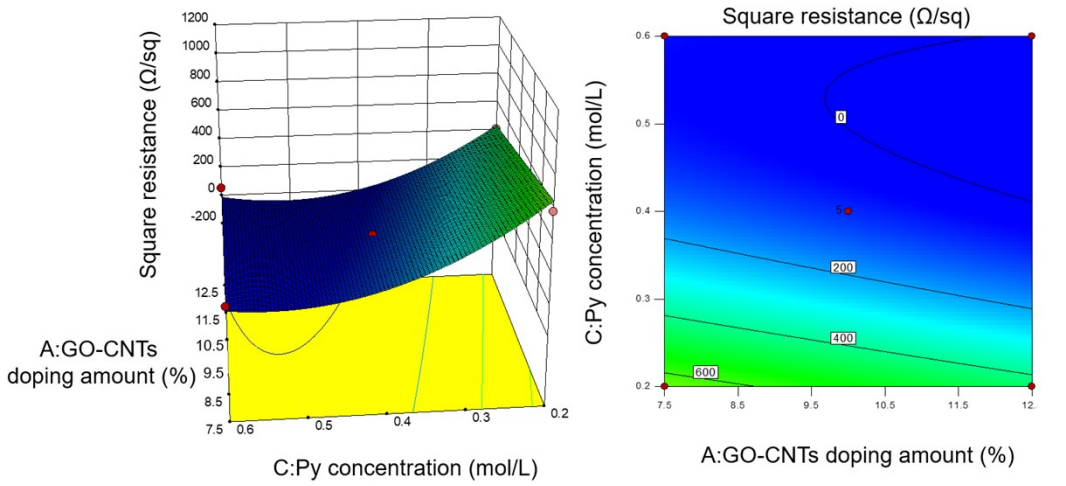

33

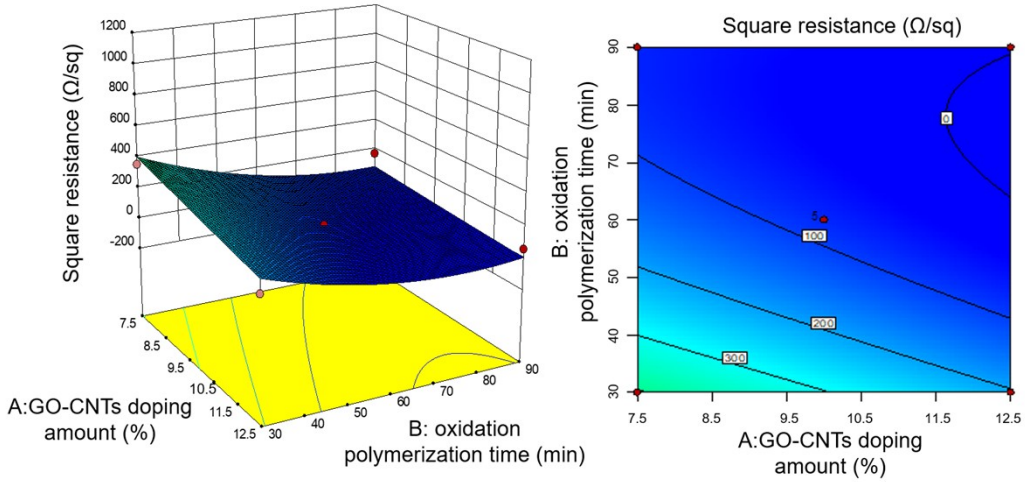

34

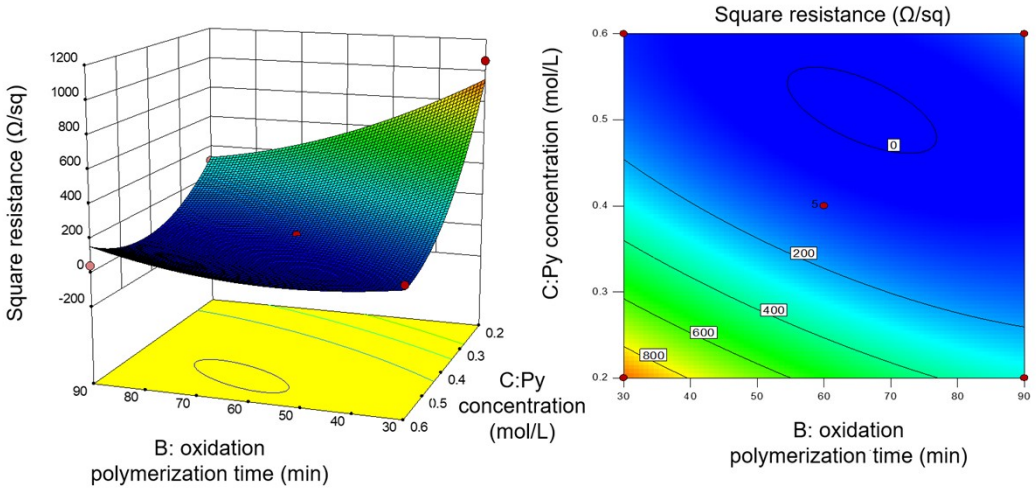

35

36 **Fig. S2.** 3D response surface for Quadratic model of square resistance

37

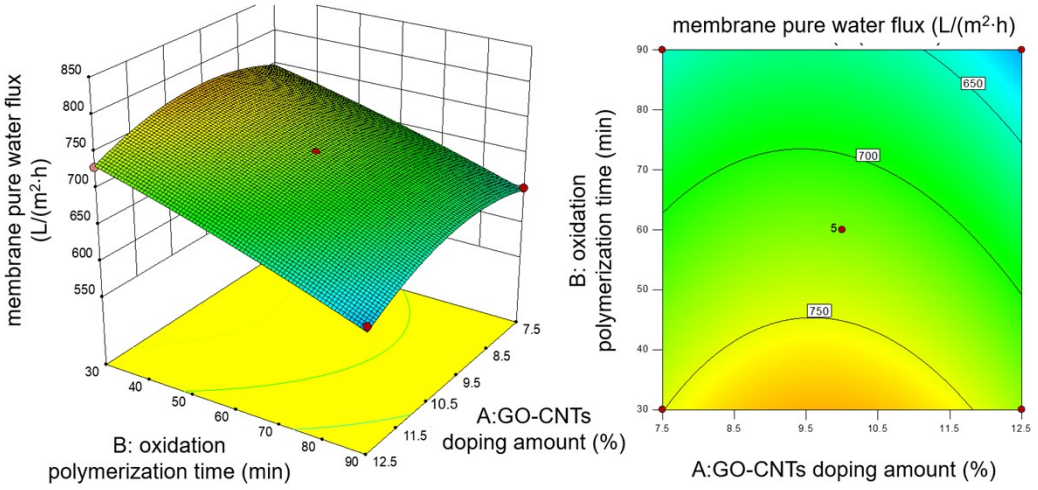

38

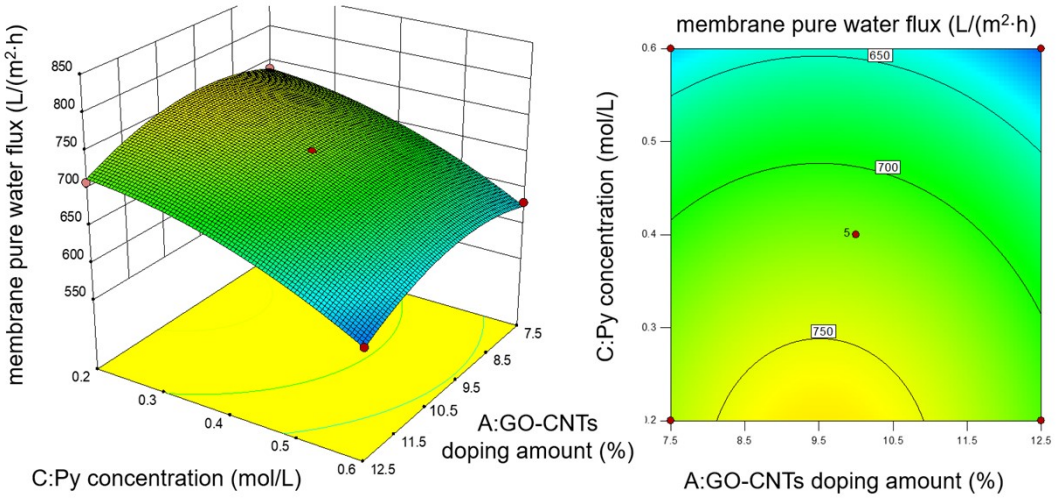

39

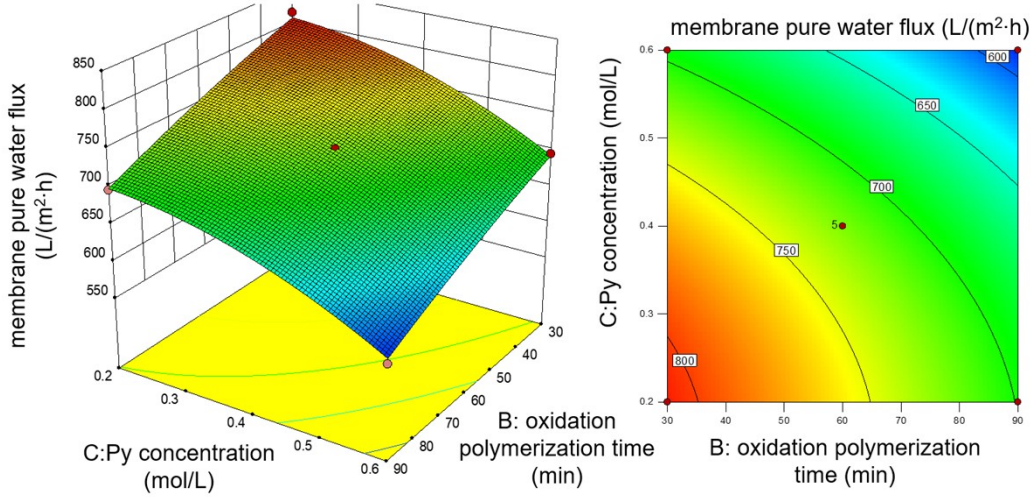

40

41 **Fig. S3.** 3D response surface for Quadratic model of membrane pure water flux

Fig. S4 shows the changes in the crystal structure of the membrane material before and after the modification. The diffraction peak in Fig. S4a is relatively sharp, indicating the existence of a relatively well-grown crystal structure on the surface of the membrane material. The analysis by Jade software reveals that the original ceramic membrane substrate surface is mainly composed of Al_2O_3 crystals and contains a small amount of SiO_2 and ZrO_2 crystals. In the XRD spectrum of the modified conductive ceramic composite membrane surface (Fig. S4b), it can be found that the broad and comprehensive diffraction peak near 2θ of 24° is the characteristic diffraction peak of PPy, which indicates that the PPy of the membrane surface has an amorphous and amorphous structure. The weak dispersion peaks near 2θ of 26° and 44° are rGO and CNTs diffraction peaks [48], indicating that rGO and CNTs are successfully doped into the PPy structure. After modification by rGO-CNTs-PPy, the diffraction peaks of Al_2O_3 and SiO_2 disappeared, suggesting that rGO-CNTs-PPy is cross-linked with Al_2O_3 and SiO_2 crystals to form a three-dimensional mesh structure.

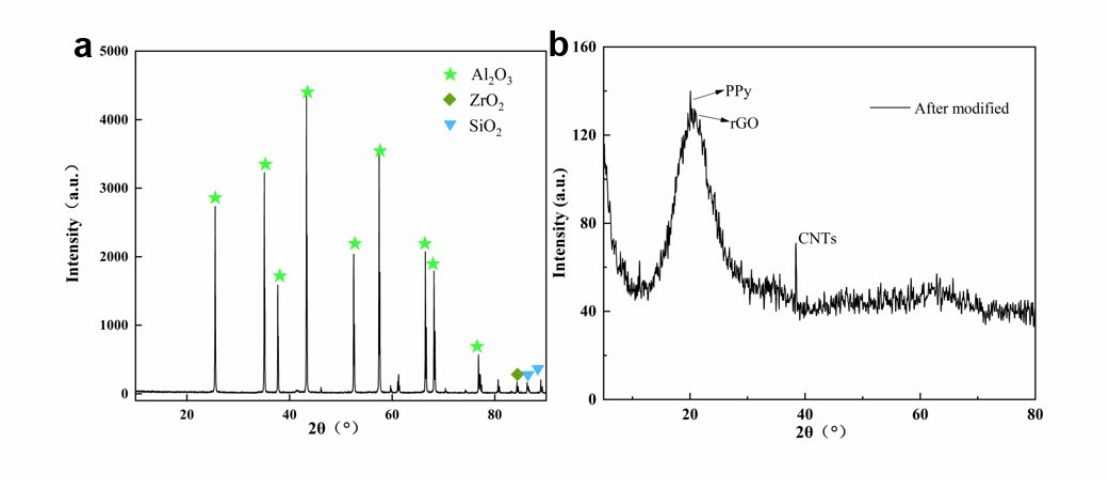

Fig. S4. (a, b) XRD image of ceramic membrane before and after modification.

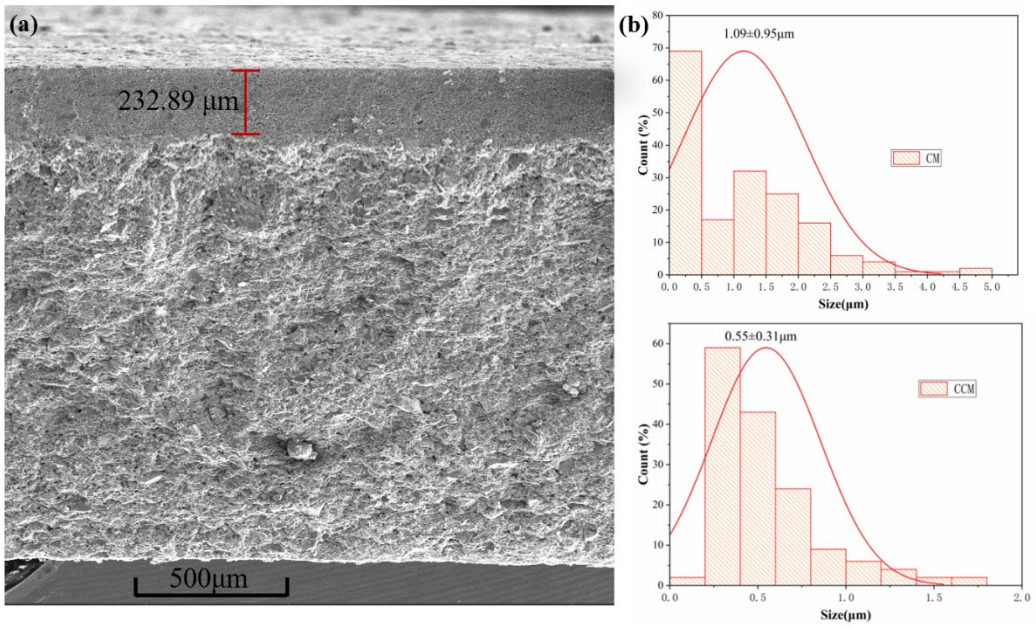

Fig. S5. (a) SEM image of modified ceramic membrane cross-section; (b) Pore size distribution of ceramic and modified ceramic membranes.